# Mineral composition of hypothermally induced ankylosis in rat molars

A report submitted in Partial Fulfilment of the requirement for the degree of Doctor of Clinical Dentistry (Orthodontics)

By

Albert Leung
B.D.S. USyd (Hons)


Orthodontic Unit
Dental School
Faculty of Health Science
The University of Adelaide
South Australia
AUSTRALIA

**2009**

# 8. ARTICLE 2

# Histological study of pulpal adaptation in an aseptic root resorption model


Doctor of Clinical Dentistry (Orthodontics)

Article 2

Written in the format for submission to:

The Journal of Dental Research

Albert Leung
B.D.S USyd (Hons)

Orthodontic Unit
Dental School
Faculty of Health Science
The University of Adelaide
South Australia
AUSTRALIA
2009

**ABSTRACT**

The aim of this pilot study was to perform a qualitative evaluation of histological alterations of the pulp tissue subsequent to an experimental thermal insult to rat molars and to demonstrate the utility of the aseptic root resorption model in pulpal regeneration evaluation. Twenty-eight, eight week old Sprague Dawley rats were divided into four groups of seven animals corresponding to one of four observations periods i.e.: $t_1$= 7 days, $t_2$= 14 days, $t_3$= 21 days, $t_4$= 28 days. At t=0 days, six animals in each group received a thermal insult, a continuous 20 minute application of dry ice ($CO_2$ at -81$^0$C) to the crowns of their upper right maxillary molar. The untreated left molars were used as controls. The remaining rat within each group did not receive the dry ice. All rats were given two sequential bone labels, calcein 5mg/kg and alizarin red 30mg/kg, administered intraperitoneally eight days apart. The timing of the labels was such that all rats were euthanased two days after the last label. Following sacrifice, the maxilla was dissected out, fixed in ethanol and embedded in methylmethacrylate. Ten microns thick, undecalcified maxillary first molar coronal sections through the furcation were obtained. For every 3 out of 10 sections: the first was left unstained and undecalcified; the second stained with Von Kossa/haematoxylin & eosin; and the third decalcified and stained with haematoxylin & eosin. Unstained sections were viewed under fluorescence, while transmitted light microscopy was used for the other sections Following initial analysis, the unstained, un-decalcified sections were de-coverslipped and carbon coated. Sections of interest were investigated with scanning electron microscopy and EDS element analysis to determine both pulpal response and tertiary dentine formation.

The results demonstrated alteration of the odontoblast layer, reduction in cellularity, vascular alterations and tertiary dentin formation. At the 28 day observation period, the cellular and vascular changes had returned to levels comparable to the control teeth. Pulp chambers were visibly smaller due to tertiary dentine formation; however, pulp necrosis was not observed. Thus it may be concluded that the aseptic root resorption model, using a continuous 20min application of dry ice, yielded reversible pulpal tissue alterations compatible with sterile inflammatory repair process.

## INTRODUCTION

The dentine-pulpal complex has an intrinsic capacity for healing and repair against a variety of tooth injuries such as caries, attrition, abrasion, and dental procedures including cavity preparation. Orthodontic tooth movement has also been demonstrated to have effects on the dental pulp (Anstendig and Kronman, 1972; Brodin et al., 1996; Derringer et al., 1996; Popp et al., 1992; Raiden et al., 1998; Ramazanzadeh et al., 2009; Santamaria et al., 2006; Santamaria et al., 2007; Subay et al., 2001; Unsterseher et al., 1987).

Odontoblasts are unique post-mitotic cells that, during tooth formation, are responsible for the synthesis and secretion of the specialized mineralized matrix of primary dentine (D'Souza et al., 1995). They remain metabolically active in a functional tooth. Secondary dentine is formed after root formation is complete, normally after the tooth has erupted and is functional. It grows much slower than primary dentine, but maintains its incremental aspect of growth. It has a similar structure to primary dentine, although its deposition is not always even around the pulp chamber (Nanci and Ten Cate, 2008). Injury induces destructive changes in odontoblasts at the affected site as well as an acute inflammatory reaction. Often the odontoblasts are injured or destroyed (Ohshima, 1990). Repair in the dentine-pulp complex often occurs as tertiary dentine formation, represented by dentine matrix being laid down at specific loci at the pulp-dentine interface in response to environmental stimuli (Smith et al., 1995). Two forms of tertiary dentine have been recognized and defined (Smith et al., 1994):

1. Reactionary dentine: a tertiary dentine matrix secreted by surviving post-mitotic odontoblast cells in response to an appropriate stimulus.
2. Reparative dentine: a tertiary dentine matrix secreted by a new generation of odontoblast-like cells in response to an appropriate stimulus, after the death of the original post-mitotic odontoblasts responsible for primary and physiological secondary dentine secretion.

The aseptic root resorption model developed by Dreyer et al. (2000) involving hypothermic injury, has been used to initiate an aseptic inflammatory response within the periodontal ligament (PDL). It was considered that the model would permit investigation of the cellular aspects of tooth root resorption without the need for intricate orthodontic mechanical systems. It has been shown to produce ankylosis and root resorption within the interradicular area of rat molar teeth at the day 14 and day 28 observation period (Chang, 2008; Di Iulio, 2007; Shaboodien, 2005). These investigations focused primarily on the adaptations within the PDL. However, following application of the cold stimulus to the occlusal surfaces of rat molars, clearly discernable changes were observed within the coronal pulp chambers of the experimental teeth. These included discontinuity of the odontoblastic layer, increased vascularity, and reduced cellularity. Considerable mineralized tissue formation was noted on the pulpal walls, which increased over time and resulted in reduced size of the pulp chamber. It was thought to be part of the protective/healing mechanism of the pulp. The cellularity and vascularity of the tissue returned to levels similar to that of the corresponding control tooth over time. It was concluded that the thermal stimulus did not cause necrosis of all cells within the pulps of

the experimental teeth and that the remaining viable cells were capable of proliferating, resulting in a healing of the pulp.

The aim of this pilot study was to perform a qualitative evaluation of histological alterations of the pulp tissue subsequent to an experimental thermal insult to rat molars and to demonstrate the utility of the aseptic root resorption model in pulpal regeneration studies.

## MATERIALS AND METHODS

Upper left and right first molars of rats from a previous experimental study, on interradicular mineralized tissue adaptation, were used (Chang, 2008). This experiment was approved by the Ethics Committee of The University of Adelaide under ethics number M-054-2006.

Twenty-eight eight week old Sprague Dawley rats were randomly divided into four groups of seven animals corresponding to one of four observations periods i.e.: $t_1$= 7 days, $t_2$= 14 days, $t_3$= 21 days, $t_4$= 28 days. At t=0 days, six animals in each group received a continuous 20 minute application of pellets of dry ice ($CO_2$ at -81$^0$C, BOC Gases, Adelaide, Australia), under anaesthesia, to the crowns of their upper right first maxillary molar. The left maxillary first molar served as controls. One rat from each group did not undergo thermal injury and represented experiment shams. All rats were given two sequential bone labels, calcein 5mg/kg and alizarin red 30mg/kg, administered intraperitoneally eight days apart. The timing of the labels was such that all rats were euthanized two days after the last label. The four groups of seven animals were each sacrificed via $CO_2$ asphyxiation at 7, 14, 21, 28 days respectively after the application of the dry ice. The maxilla was dissected out, trimmed, and fixed in 70% ethanol. Tissue dehydration and defatting was performed prior to embedding in methylmethacrylate. Ten microns thick serial, coronal sections were cut, with a Reichert-Jung microtome (Leica Microsystems GmbH Wetzlar, Germany), through the furcation region of the upper first molar teeth. For every 3 out of 10 sections: the first was kept unstained and undecalcified; the second stained with Von Kossa/haematoxylin & eosin; and the third decalcified and stained with haematoxylin & eosin. Unstained sections were viewed

under fluorescence, while transmitted light microscopy was used for the other sections following initial analysis, the unstained, un-decalcified sections were de-coverslipped, by soaking in xylene, and carbon coated. These sections were investigated with a Philips XL30 FEG Scanning Electron Microscope (SEM) at 15kV using the backscattered electron detector (BSE). Qualitative and quantitative elemental analysis of mineral tissue in the pulp was carried out by Energy dispersive x-ray analysis (EDS) with an EDAX DX4 detector (EDAX, USA). Measurements were taken under the following conditions: acquisition time of 100 live seconds, accelerating voltage 10kV, count rate of 1800-2000 counts per second, dead time of 20-30% and working distance 10mm.

**RESULTS**

Under light microscopy, changes in response to the thermal insult were observed in both the pulp and PDL. Over time, there was a cumulative decrease in the size of the pulp chamber on the right molar of the treatment rats, as a result of the deposition of mineralized tissue along the walls of the pulp chamber. The difference in size between the left and right first molar pulp chambers was particularly noticeable in the 28 day treatment rats. Vascularity and numbers of blood vessels in the pulp chamber increased until 14 days and then reduced. Decreased cellularity was seen initially at day 14 with a return to levels similar to controls at day 28.

Changes in the PDL, with regards to mineral tissue apposition rates, PDL width and resorptive surfaces, was examined as part of another study (Chang, 2008). The author observed an initial spike during day 14 in mineral tissue apposition rates along the bone and root surface. This declined to levels of the control teeth by day 28. Resorption levels along the root surface remained significantly elevated at day 28. The significantly wider PDL width in the treated molars showed a declining trend towards that of the control teeth by day 28.

Definite ankylosis was observed in the upper right first molars of 3 experimental animals: two at 14 days and one at 21 days. Ankylosis was not seen in any of the sham rats or in any of the control molars of the treated rats.

At day 7, the pulp chambers of the experimental teeth (Figure 1) were much less cellular, with relatively sparse nuclei, compared to the control molars (Figure 2). The odontoblast layer of cells was either absent or reduced in numbers in most treatment molars. There

was a loss of cellular polarity and arrangement as a sheet of cells. Cell numbers were sparser with a reduction in basophilic structures in comparison to the control teeth; this indicated incomplete lysis of the odontoblastic layer. Increased vascularity, with numerous small blood vessels was noted within the pulp chamber of the right molars. The blood vessels were located within the vicinity of areas where there was discontinuity and changes in the odondoblast layer. In one rat, polymorphonuclear leukocytes with intensely staining nuclei were observed in the pulp, indicating that an acute inflammatory reaction had occurred.


**Figure 1. Day 7, right molar, VK/H&E stain.** Increased vascularity within the pulp chamber was a common finding in the treated molars. Disrupted odontoblast layer with loss of polarity and reduced cellularity (asterisk) BV: Blood vessels, PP: Pulpal-periodontal canal. Scale bar = 500µm.

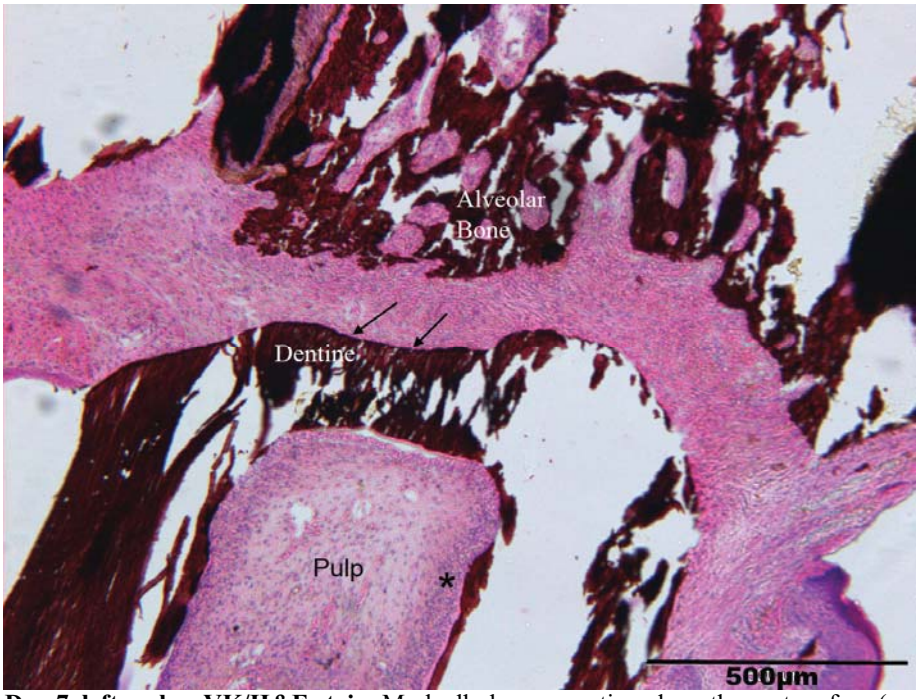


**Figure 2. Day 7, left molar. VK/H&E stain.** Markedly less resorption along the root surface (arrows). Asterisk shows a well defined continuous zone around the pulpal walls resembling odontoblasts. These features were common to all control molars in treated and sham rats. Scale bar = 500µm.

At 14 days following thermal injury, a layer of atubular mineralized tissue had formed around the peripheries of the dental pulp. Following this was a layer of unmineralised pre-dentine matrix lined by odontoblast-like cells (Figures 3 and 4). The mineralised tissue displayed characteristics of tertiary dentine. Similar to pulps at day 7, increased vascularity and vasodilatation were seen around the peripheries where tertiary dentine was present.

Where ankylosis was observed in the PDL, an area devoid of odontoblasts was seen (Figure 3, 5 and 6). Deposition of bone-like tissue was seen away from the lateral wall of the pulp and radiating in towards the central area of the pulp. A concentration of haematoxyphilic cells lined the surfaces of this tissue and the adjacent blood vessels. These cells appeared to have odontoblast-like qualities with an oval nucleus and haematoxyphilic (basophilic) cytoplasm. Fluorescent light microscopic examination of the adjacent unstained section revealed concentration of alizarin red label around the periphery of the pulp as well as in the bone-like tissue (Figure 7), indicting that mineral

apposition had occurred simultaneously. BSE imaging of the same slide allows for identification and confirmation of the presence of mineralized tissue within the pulp (Figures 8 and 9). The bone-like tissue, as identified in H&E stained sections and unstained sections under fluorescence microscopy, appeared as many fine foci of calcification as well as clusters. These calcified bodies were located away from the pulp-dentine interface, and as such may not be directly associated with tertiary dentine formation. New mineral apposition along the neighbouring pulpal wall also displayed an atubular appearance (Figure 9).

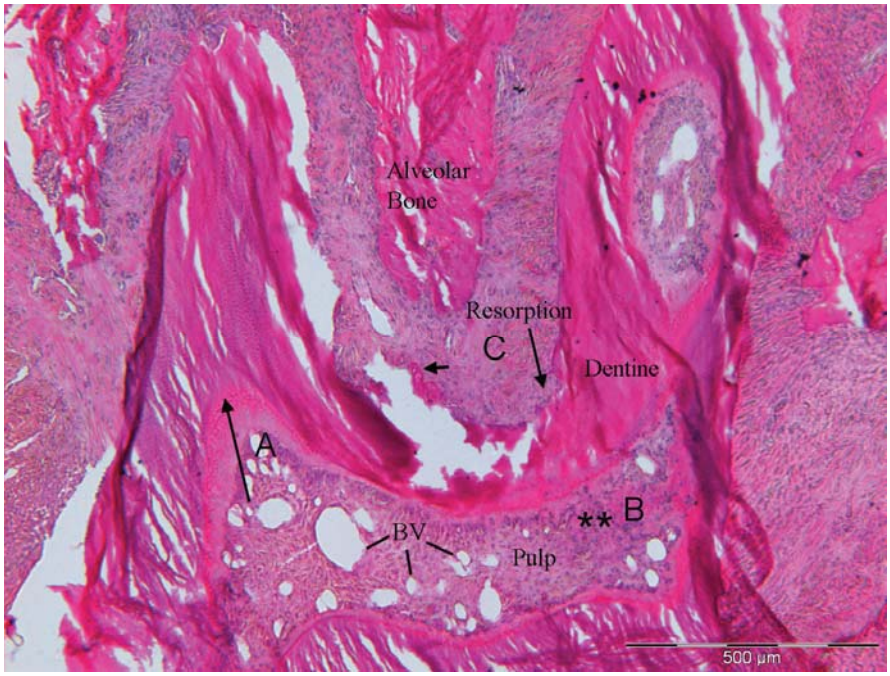


**Figure 3. Day 14, right molar. H&E stain. Root resorption with repair cellular cementum-like tissue formation on the root surface, concurrent with marked localized cellular and vascular changes in the pulp, including bone-like tissue (**).** No odontoblast layer is visible adjacent to the bone-like tissue. Higher power views of regions A and B are shown in Figures 4 and 5. Small arrow: the cellular cementum-like tissue on root surface. Long arrow: amorphous mineralized tissue resembling tertiary dentine. BV: Blood vessels. Scale bar = 500µm.

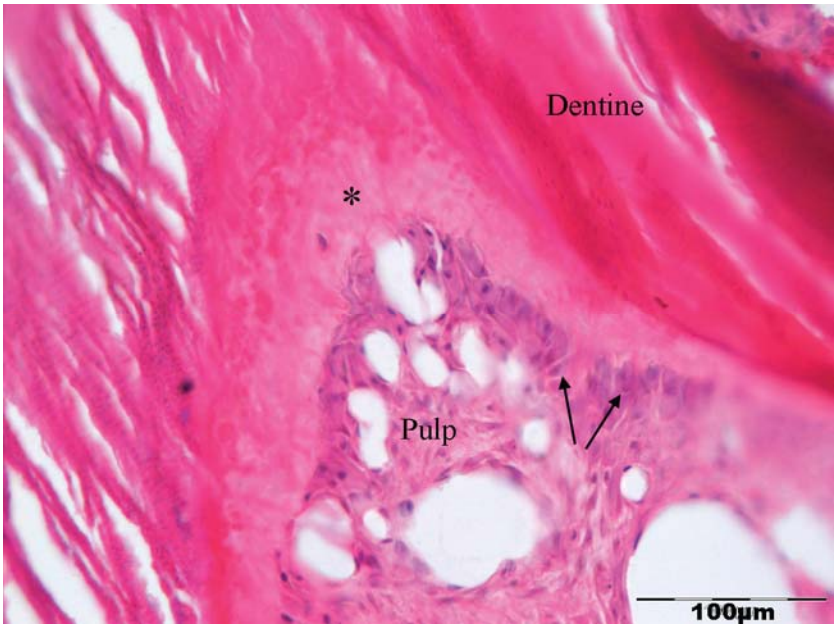


**Figure 4. Higher power view of Region A in pulp chamber in Fig 3.** Odontoblast layer (arrows) lying deep to a wide layer of unmineralised predentinal matrix (asterisk).

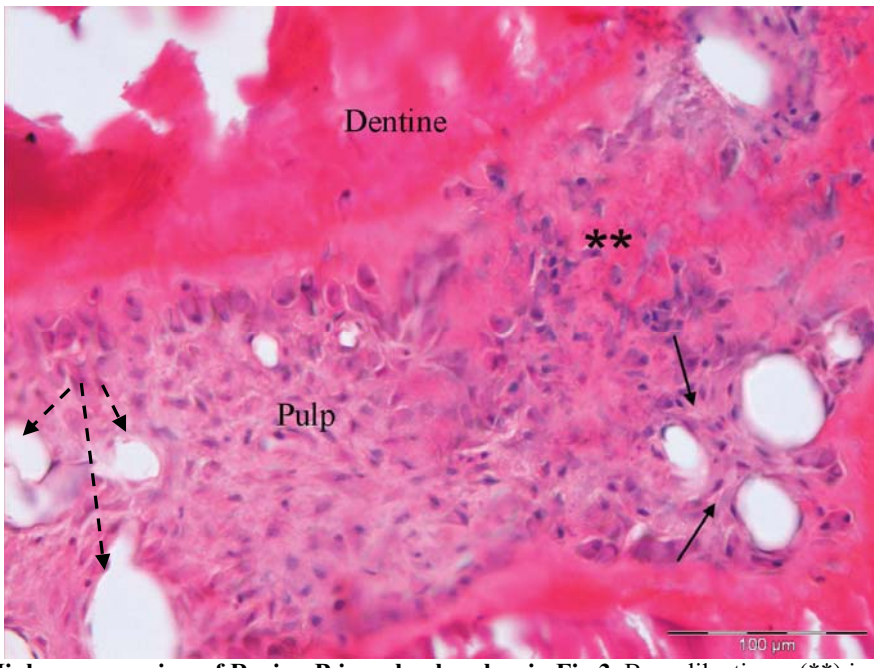


**Figure 5. Higher power view of Region B in pulp chamber in Fig 3.** Bone-like tissue (**) in pulp chamber surrounded by haematoxyphilic cells. The vascular pericytes close to this bone-like tissue are a rim of haematoxyphilic cells (unbroken arrows) which is absent around the blood vessels (broken arrows) in the left of this micrograph, distant from the bone-like tissue. Scale bar = 100µm.

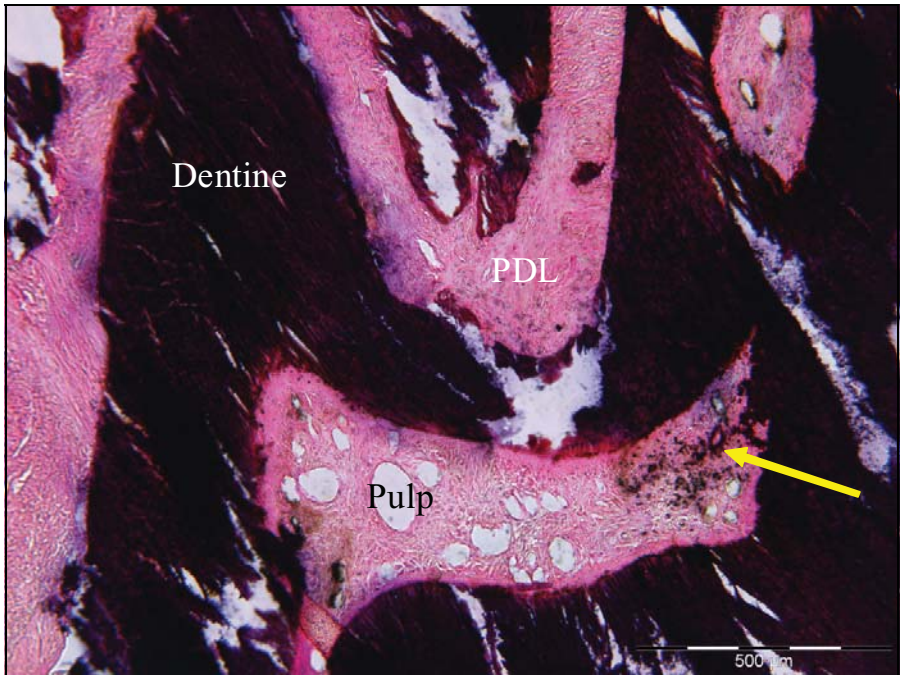


**Figure 6. Day 14, right molar, VonKossa/H&E stain.** Bone-like nodules are stained black (yellow arrow). There is an unmineralised layer of predentine matrix lining the pulpal walls. Scale bar = 500µm.

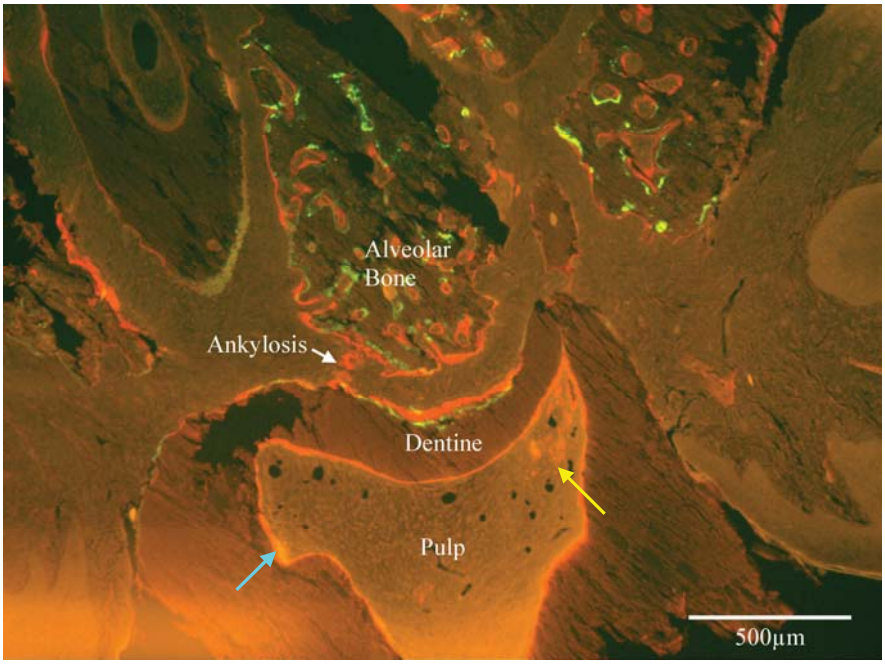


**Figure 7. Day 14, right molar. Unstained.** Mineralisation in the pulp characterised by a concentration of alizarin red (yellow arrow). Mineral apposition has also occurred around the periphery of the pulp chamber (blue arrow). Ankylosis is present with rapid apposition across the periodontal ligament space. (White arrow).

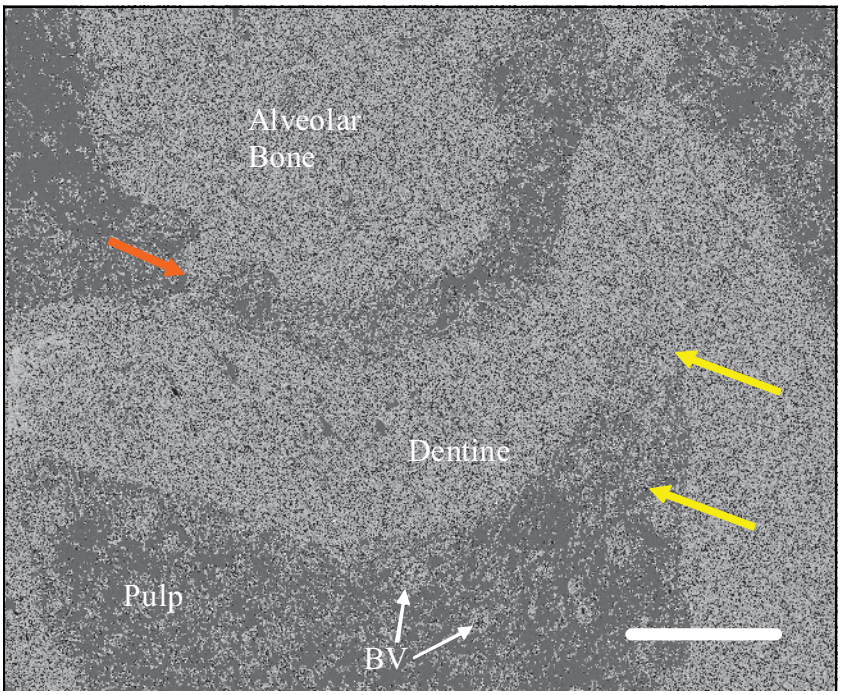


**Figure 8. Day 14, right molar, Unstained, BSE image, scale bar 200µm.** Surfaces with a high mean atomic number appear lighter. This allows identification of mineralized tissues within the pulp chamber. Bone-like tissue (yellow arrows), as identified in previous slides, appears nodular and without structural organization. Ankylosis (red arrow) is also visible on this slide

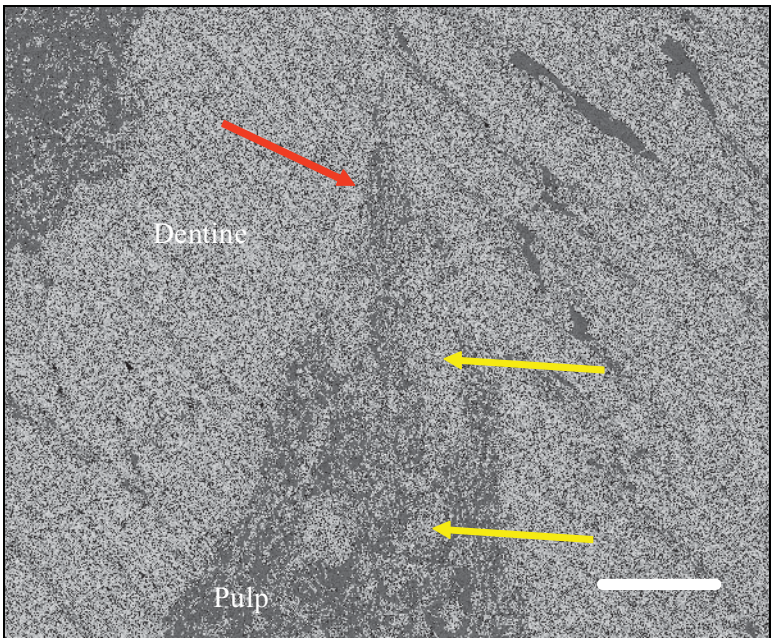


**Figure 9. Day 14, right molar, Unstained, higher magnification BSE image of bone-like tissue (yellow arrows). Scale bar 50µm.** Bone-like tissue appears as multiple, fine focal nodular formations coalescing together without any structural organization. Tertiary dentine (red arrow) on pulpal wall displays an atubular structure relative to primary dentine.

EDS x-ray microanalysis was performed on the calcific bodies seen in Figure 10. Qualitative and quantitative analysis revealed calcium and phosphorus as the major elements, with trace amounts (<1% weight) of magnesium and sodium. The Ca/P ratio was 2.01, thus indicating that the bodies were composed of calcium phosphate in apatite form.

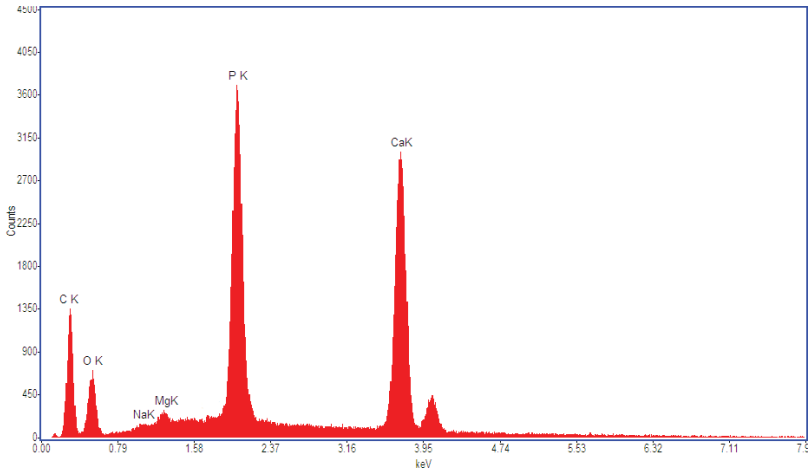


**Figure 10. EDS data of a spot scan in bone-like tissue within the pulp.** Strong peaks were shown of Ca, P, O and C, with lower peaks for Na and Mg. Day 14, Rat 3. 10kv, 100 live seconds, working distance 10mm

At day 21, increased vascularity continued to be seen in the treatment molars relative to the controls but the numbers of blood vessels within the pulp were less than at day 14. Tertiary dentine had continued to be deposited. The odontoblast layer and the central pulp space still displayed reduced cellularity relative to controls. More pronounced bone-like tissue was observed in some rats (Figures 11 and 12). The location was toward the lateral walls of the pulp, similar to the calcified foci observed at day 14. In one rat, bone-like tissue had invaded the central pulpal space, it was adherent to and continuous with tertiary dentine (Figures 12 and 13). The morphology was of a disorganized, atubular appearance and surrounded by unmineralised pre-dentine matrix. Cells were seen trapped amongst the bone-like tissue and surrounded by unmineralised osteoid. Reactive hard tissue deposition was also observed within the PDL. However, no ankylotic bridging was present. Sham rats and control teeth displayed no reactive cellular hard tissue deposits on the root surface or the pulpal walls.

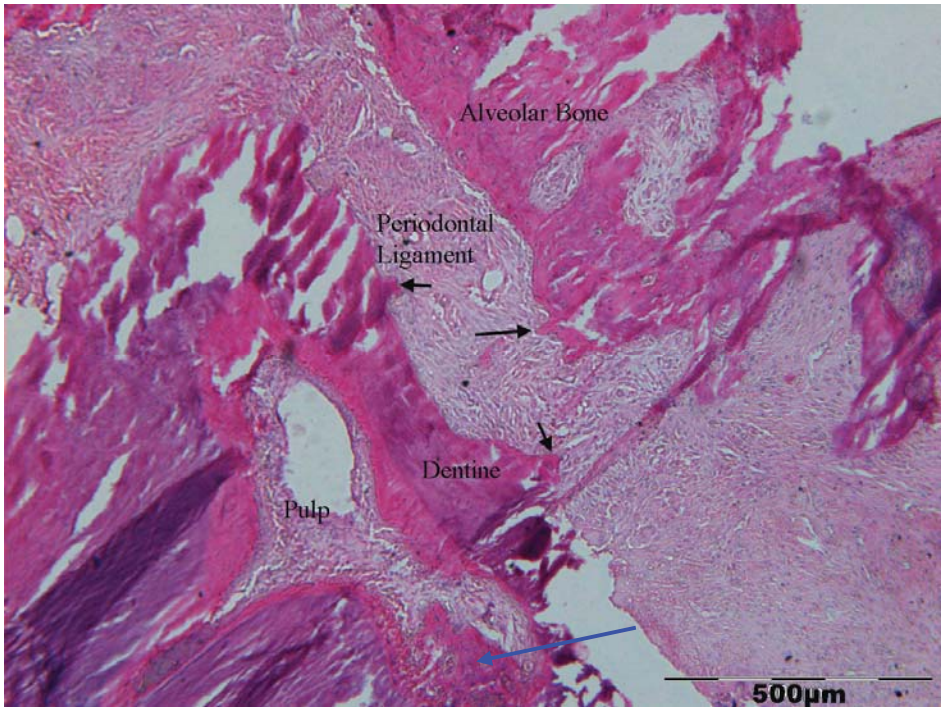


**Figure 11. Day 21, right molar. H&E stain.** Tertiary dentine seen around the periphery of the pulp chamber. Bone-like tissue with cellular inclusions extending into the central pulp space (blue arrow). No ankylosis present but irregular extensions from bone and root surface (black arrows) and bone –like tissue within the middle of the periodontal ligament. Scale bar = 500µm.

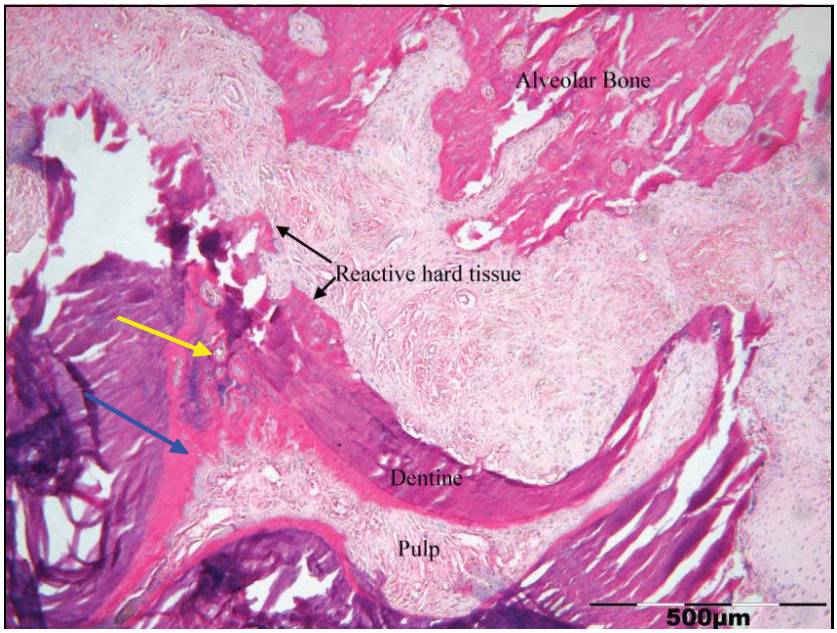


**Figure 12. Day 21, right molar, H&E stain.** More pronounced bone-like tissue within the pulp chamber (blue arrow). A single cell with a single nucleus could be seen within the bone-like tissue and surrounded by unmineralised predentine matrix (yellow arrow). A thicker layer of predentine matrix was also a feature at 21 days (blue arrow). Concurrent reactive hard tissue deposition is present within the PDL (black arrows). Scale bar = 500µm.

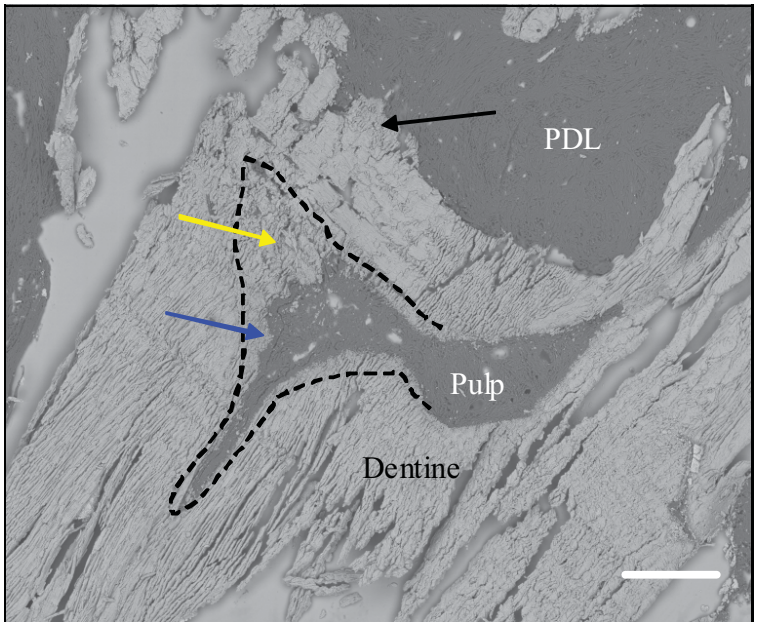


**Figure 13. Day 21, right molar, BSE image.** Scale bar = 200µm**.** Tertiary dentine is outlined by dotted line. The morphology of the bone-like tissue (yellow arrow) does not display the same tubular characteristic of dentine. Tertiary dentine also displays an atubular nature (blue arrow). Concurrent reactive hard tissue on the tooth side of the PDL (Black arrow)

By day 28, further development of tertiary dentine had occurred. The pulp chambers of the treatment teeth were considerably smaller compared to controls (Figures 14 and 16). The most recent tertiary dentine formed was tubular in appearance. This feature was not consistent along the entire thickness of tertiary dentine. Tertiary dentine closer to physiological dentine appeared atubular with some areas displaying lace-like (Figure 15) and globular morphology (Figure 16). In some rats, the tertiary dentine layer was considerably thicker in localized areas. These were located at the lateral walls, corresponding with the bony material observed at day 14. These areas were atubular throughout the entire thickness. The odontoblastic layer also re-established itself with cellularity similar to that of control teeth. They completely lined the pulpal walls, including the localized thicker areas. The vascular reactive response to the initial thermal insult was less, as fewer blood vessels were noted in the pulp chamber compared with the preceding three time periods, although this may be partly due to the smaller size of the pulp chamber seen in the treated teeth. These features suggested signs of pulpal repair after the initial freezing insult.

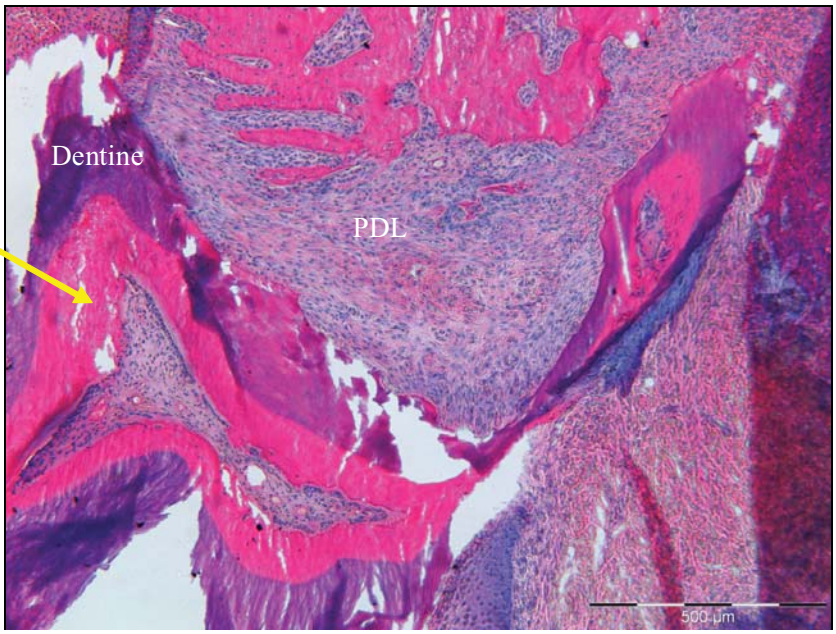


**Figure 14. Day 28, right molar. H&E stain.** Scale bar = 500µm. Fewer blood vessels in the pulp compared with earlier time periods (Figs 1 and 3), lined by a rim of odontoblast-like cells, which lie beneath a wide zone of tertiary dentine (yellow arrow).

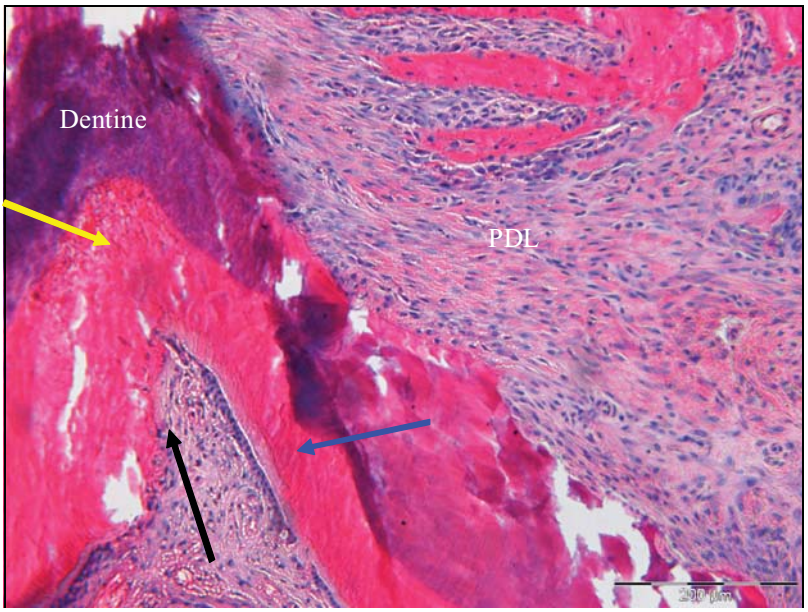


**Figure 15. Day 28, right molar. H&E stain.** Scale bar = 200µm**.** A closer view of the tertiary dentine. Tertiary dentine without dentine tubules and lace like appearance (yellow arrow). In localised areas, reduced numbers of odontoblasts were seen adjacent to the atubular dentine (black arrow). A second type of tertiary dentine was observed (blue arrow) with parallel tubules and lined by a uniform layer of odontoblasts. The tubules did not appear to traverse the entire span of tertiary dentine, or appear continuous with the primary dentine. Scale bar = 200µm**.**

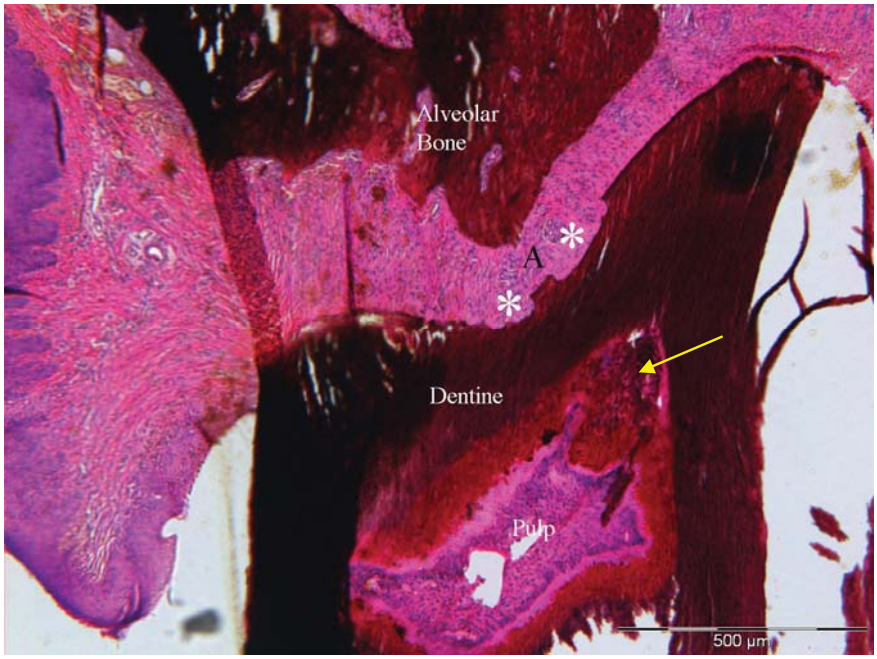


**Figure 16. Day 28, right molar. VK/H&E stain.** Scale bar = 500µm**.** A cellular pulp with tertiary dentine staining less intensely than surrounding dentine. Tertiary dentine is variable in nature with lace like concentrations of mineral (yellow arrow). Irregular root surface (asterisks) characteristic of resorption was also present in the periodontal ligament.

## DISCUSSION

The early increase in the number and size of small blood vessels, observed at day 7, could be due to an initial vasodilatation during the initial stages of an inflammatory process and new microvessel formation(Grunheid et al., 2007). External noxious stimulus results in degranulation of mast cells, causing biochemical reactions and release of inflammatory mediators of inflammation e.g. histamine, bradykinin, neurokines, neuropeptides, prostaglandins and growth factors (Santamaria et al., 2007). These mediators generally induce vasodilation, increase in blood flow and vascular permeability, and oedema. The aim of this vascular change is to provide the inflammatory cells to the area, as well as to ensure that the bacterial toxins and metabolic waste products are eliminated from the area (Tjaderhane, 2002). At later observation periods, the number and size of blood vessels had reduced to levels similar to the control and sham teeth, indicating that vascular supply to the pulp was not irreversibly compromised by the thermal insult.

A variety of changes to the odontoblast layer was observed over time. Some odontoblasts exhibited alterations in form with distended nuclei and diffuse chromatin, suggesting a change in metabolic activity (Santamaria et al., 2007). There was also a reduction in cellularity of the odontoblastic layer at 7 days. By 28 days the cell metabolism, altered by the inflammatory process with presence of oedema and signs of vascular changes, had returned to levels comparable to controls. This demonstrated the capability of pulpal repair.

The reactive hard tissue formation formed throughout the experiment had characteristics of tertiary dentine. Tertiary dentine is generally recognized as representing a dentine

matrix laid down at specific loci at the pulp-dentine interface in response to environmental stimuli. It is classified with regards to the cells responsible for laying down dentine. Reactionary dentine is produced by surviving post-mitotic odontoblast cells in response to a mild injury. Reparative dentine is a tertiary dentine matrix secreted by a new population of odontoblast-like cells in response to an intense type of injury such as traumatic events or deep cavity preparations (Smith et al., 1995). The structure of tertiary dentine is very variable with a spectrum appearance ranging from a regular, tubular matrix similar to that of primary dentine to a very dystrophic, atubular matrix possibly containing cells trapped within.

Based on the atubular morphology of the initial tertiary dentine seen in this study, it is believed that a predominantly reactionary dentine response was seen in most rats. True classification of tertiary dentine is difficult in this study as the first observation day was day 7. Experiments of pulpal wound healing via cavity preparation indicate that necrosis and replacement of odontoblasts by differentiation of progenitor cells in the sub-odontoblastic layer is complete by 72 hours (Harada et al., 2008). Progressive mineralized tissue deposition through to day 28 and an absence of resorption were seen, concurrent with a decrease in the physical size of the pulp chamber. Resorption of extensive mineralized deposits within the pulp has been observed to occur between 60 to 120 days in replanted rat molars (Komatsu et al., 2008). Resorption within the pulp is more likely to occur with replantation injuries, where the apical blood supply has been severed (Yu and Abbott, 2007). As such, the absence of resorption within the pulp chamber in this study may be related to the mild nature of the thermal insult and the time of observation.

In one rat, at day 14, bone-like tissue surrounded by haematoxyphilic cells was observed in the region of the pulp where the odontoblast layer was discontinuous. The mineralized tissue consisted of multiple focal areas of calcified material, as confirmed by BSE. These nodules were sparsely distributed and separate from the pulp-dentine walls. The absence of an odontoblastic-like layer and the location of these nodules suggest that their development may be part of a process unrelated to tertiary dentine formation. EDS x-ray analysis confirmed the calcified material being composed of mainly calcium and phosphorus. With the absence of odontoblasts, it is postulated that this calcified material is a product of osteogenic cells which have differentiated from a precursor population of cells during the process of pulpal repair (Smith et al., 1995). The origins of these progenitor cells are still unknown. Potential derivations of suggested cells include the cell-rich layer of Höhl adjacent to the odontoblasts, perivascular cells, undifferentiated mesenchymal cells and fibroblasts (Sloan and Smith, 2007). An in vitro study showed that pulp fibroblasts cultured from human deciduous and supernumerary teeth formed crystals with an X-ray diffractometry pattern consistent with hydroxyapatite (Tsukamoto et al., 1992), thus showing that fibroblasts themselves could produce calcific changes. More recently, the presence of a unique population of post-natal dental pulp stem cells (DPSC) has been reported (Gronthos et al., 2000; Gronthos et al., 2002; Huang et al., 2008; Sloan and Smith, 2007; Sloan and Waddington, 2009; Suchanek et al., 2009). The DPSCs have been found to express the perivascular cell marker CD146, amongst other markers which have been co-localized to perivascular sites in the pulp (Shi and Gronthos, 2003). In another study, human DPSCs, characterised by mesenchymal stem cell marker Stro-1, were isolated from dental pulps of third molars and cultured in

neurogenic, osteogenic/odontogenic, adipogenic, myogenic, and chondrogenic inductive media. Immunohistochemistry and reverse transcriptase-polymerase chain reaction (RT-PCR) analysis revealed that the DPSCs had the capability to differentiate into more pathways than their origin; such as the neuron-, odontoblast-, adipocyte-, myoblast-, and chondrocyte-like phenotypes (Zhang et al., 2006).

In the current study, blood vessels adjacent to the bone-like material were lined by haematoxyphilic cells. These cells were not seen around other blood vessels away from the bone-like material in the same section. Thus the odontoblast-like cells that formed the bone-like tissue may have been derived from the vascular pericytes which may be of stem cell origin.

Ankylosis was also present in the rat which displayed bone-like tissue within the pulp. This phenomenon was also noted in other studies using a tooth replantation model (Komatsu et al., 2008; Nishioka et al., 1998). This suggests the need for a stronger noxious stimulus.

The aseptic root resorption model, involving hypothermic injury, was developed to initiate an aseptic inflammatory response within the PDL (Dreyer et al., 2000). The authors observed the occlusally applied cold thermal stimulus caused degeneration of the adjacent structures of the PDL by cell death. Thermal stimulus on extracted teeth causes hydrodynamic fluid movement which occurs before the temperature changes at the pulpal wall, due to low thermal conductivity (Dreyer, 2002). This flow can be bidirectional and may not be solely due to expansion and contraction of fluids, enamel expansion or contraction can also occur, exerting a physical effect on mechanical fluid movement

within the pulp (Linsuwanont et al., 2007). Changes in hydrostatic pressure within the pulp can also occur during chronic parafunctional forces from clenching and bruxism, resulting in pulpal inflammation, elevated intrapulpal pressure and deposition of calcified nodules (Yu et al., 2009). Orthodontic tooth movement has been shown to affect vascular and blood flow changes with increases in volume density of pulpal blood vessels within 6 hours of orthodontic tooth movement (Santamaria et al., 2006). Oedema of pulpal tissue and dilated blood vessels have also been reported in orthodontically extruded teeth (Mostafa et al., 1991). Other histological changes associated with orthodontic tooth movement include alteration of the odontoblastic layer, with hypertrophy of odontoblasts, oedema of the pulp connective tissue in the central area of the pulp, and vascular alteration with accumulation of erythrocytes and leukocytes inside the vessels (Santamaria et al., 2007). The changes to the intact odontoblastic layer at day 14, is similar to that seen at 6hrs in tooth movement models (Santamaria et al., 2007). Thus the aseptic root resorption model may be valid in the investigation of the cellular changes within the pulp as a result of tooth movement. By comparing the histological changes that occurred within the pulp to that seen during orthodontic tooth movement, it would suggest that a 20 minute dry ice insult does provoke a more pronounced response (Anstendig and Kronman, 1972; Santamaria et al., 2007). A 20 minute and higher dry ice insult would create a model suitable for investigating the healing potential of the pulp.

## CONCLUSION

The observations of this study suggest that the aseptic root resorption model, using a continuous 20 minute application of dry ice, may be capbable of producing alteration of the odontoblast layer, reduction in cellularity, vascular alterations and tertiary dentine formation. At the 28 day observation period, the cellular and vascular changes appeared to return to levels comparable to the control teeth. Pulp chambers were visibly smaller due to tertiary dentine formation; however, no pulp necrosis was observed. Thus it may be concluded that the changes are suggestive of a reversible pulpal tissue alteration compatible with an inflammatory repair process. The aseptic root resorption model may be useful in the future for studying the mechanisms underlying dentine and pulpal regeneration.

**REFERENCES**

Anstendig HS, Kronman JH (1972). A histologic study of pulpal reaction to orthodontic tooth movement in dogs. *Angle Orthod* 42(1)*:*50-5.

Brodin P, Linge L, Aars H (1996). Instant assessment of pulpal blood flow after orthodontic force application. *J Orofac Orthop* 57(5)*:*306-9.

Chang A (2008). Interradicular Mineralized Tissue Adaptation In An Aseptic Necrosis Model. Doctorate of Clinical Dentistry Thesis. Adelaide, University of Adelaide.

D'Souza RN, Bachman T, Baumgardner KR, Butler WT, Litz M (1995). Characterization of cellular responses involved in reparative dentinogenesis in rat molars. *J Dent Res* 74(2)*:*702-9.

Derringer KA, Jaggers DC, Linden RW (1996). Angiogenesis in human dental pulp following orthodontic tooth movement. *J Dent Res* 75(10)*:*1761-6.

Di Iulio DS (2007). Relationship of epithelial cells and nerve fibres to experimentally induced dentoalveolar ankylosis in rats. Doctorate of Clinical Dentistry Thesis (thesis). Adelaide, University of Adelaide.

Dreyer CW, Pierce AM, Lindskog S (2000). Hypothermic insult to the periodontium: a model for the study of aseptic tooth resorption. *Endod Dent Traumatol* 16:9-15.

Dreyer CW (2002). Clast Cell Activity in a Model of Aseptic Root Resorption. Adelaide, PhD thesis, The University of Adelaide.

Gronthos S, Mankani M, Brahim J, Robey PG, Shi S (2000). Postnatal human dental pulp stem cells (DPSCs) in vitro and in vivo. *Proc Natl Acad Sci U S A* 97(25)*:*13625-30.

Gronthos S, Brahim J, Li W, Fisher LW, Cherman N, Boyde A, et al. (2002). Stem cell properties of human dental pulp stem cells. *J Dent Res* 81(8)*:*531-5.

Grunheid T, Morbach BA, Zentner A (2007). Pulpal cellular reactions to experimental tooth movement in rats. *Oral Surg Oral Med Oral Pathol Oral Radiol Endod* 104(3)*:*434-41.

Harada M, Kenmotsu S, Nakasone N, Nakakura-Ohshima K, Ohshima H (2008). Cell dynamics in the pulpal healing process following cavity preparation in rat molars. *Histochem Cell Biol* 130(4)*:*773-83.

Huang AH, Chen YK, Lin LM, Shieh TY, Chan AW (2008). Isolation and characterization of dental pulp stem cells from a supernumerary tooth. *J Oral Pathol Med* 37(9)*:*571-4.

Komatsu K, Shimada A, Shibata T, Shimoda S, Oida S, Kawasaki K, et al. (2008). Long-term effects of local pretreatment with alendronate on healing of replanted rat teeth. *J Periodontal Res* 43(2)*:*194-200.

Linsuwanont P, Palamara JE, Messer HH (2007). An investigation of thermal stimulation in intact teeth. *Arch Oral Biol* 52(3)*:*218-27.

Mostafa YA, Iskander KG, El-Mangoury NH (1991). Iatrogenic pulpal reactions to orthodontic extrusion. *Am J Orthod Dentofacial Orthop* 99(1)*:*30-4.

Nanci A, Ten Cate AR (2008). Ten Cate's oral histology : development, structure, and function. 7th ed. St. Louis, Mo.: Mosby Elsevier.

Nishioka M, Shiiya T, Ueno K, Suda H (1998). Tooth replantation in germ-free and conventional rats. *Endod Dent Traumatol* 14(4)*:*163-73.

Ohshima H (1990). Ultrastructural changes in odontoblasts and pulp capillaries following cavity preparation in rat molars. *Arch Histol Cytol* 53(4)*:*423-38.

Popp TW, Artun J, Linge L (1992). Pulpal response to orthodontic tooth movement in adolescents: a radiographic study. *Am J Orthod Dentofacial Orthop* 101(3)*:*228-33.

Raiden G, Missana L, Santamaria de Torres E, Kozuszko S, Pedroso R (1998). Pulpal response to intrusive orthodontic forces. *Acta Odontol Latinoam* 11(1)*:*49-54.

Ramazanzadeh BA, Sahhafian AA, Mohtasham N, Hassanzadeh N, Jahanbin A, Shakeri MT (2009). Histological changes in human dental pulp following application of intrusive and extrusive orthodontic forces. *J Oral Sci* 51(1)*:*109-15.

Santamaria M, Jr., Milagres D, Stuani AS, Stuani MB, Ruellas AC (2006). Initial changes in pulpal microvasculature during orthodontic tooth movement: a stereological study. *Eur J Orthod* 28(3)*:*217-20.

Santamaria M, Jr., Milagres D, Iyomasa MM, Stuani MB, Ruellas AC (2007). Initial pulp changes during orthodontic movement: histomorphological evaluation. *Braz Dent J* 18(1)*:*34-9.

Shaboodien S (2005). Traumatically induced dentoalveolar ankylosis in rats. Adelaide, Doctor of Clinical Dentistry Thesis, University of Adelaide.

Shi S, Gronthos S (2003). Perivascular niche of postnatal mesenchymal stem cells in human bone marrow and dental pulp. *J Bone Miner Res* 18(4)*:*696-704.

Sloan AJ, Smith AJ (2007). Stem cells and the dental pulp: potential roles in dentine regeneration and repair. *Oral Dis* 13(2)*:*151-7.

Sloan AJ, Waddington RJ (2009). Dental pulp stem cells: what, where, how? *Int J Paediatr Dent* 19(1)*:*61-70.

Smith AJ, Tobias RS, Cassidy N, Plant CG, Browne RM, Begue-Kirn C, et al. (1994). Odontoblast stimulation in ferrets by dentine matrix components. *Arch Oral Biol* 39(1)*:*13-22.

Smith AJ, Cassidy N, Perry H, Begue-Kirn C, Ruch JV, Lesot H (1995). Reactionary dentinogenesis. *Int J Dev Biol* 39(1)*:*273-80.

Subay RK, Kaya H, Tarim B, Subay A, Cox CF (2001). Response of human pulpal tissue to orthodontic extrusive applications. *J Endod* 27(8)*:*508-11.

Suchanek J, Soukup T, Visek B, Ivancakova R, Kucerova L, Mokry J (2009). Dental pulp stem cells and their characterization. *Biomed Pap Med Fac Univ Palacky Olomouc Czech Repub* 153(1)*:*31-5.

Tjaderhane L (2002). The mechanism of pulpal wound healing. *Aust Endod J* 28(2)*:*68-74.

Tsukamoto Y, Fukutani S, Shin-Ike T, Kubota T, Sato S, Suzuki Y, et al. (1992). Mineralized nodule formation by cultures of human dental pulp-derived fibroblasts. *Arch Oral Biol* 37(12)*:*1045-55.

Unsterseher RE, Nieberg LG, Weimer AD, Dyer JK (1987). The response of human pulpal tissue after orthodontic force application. *Am J Orthod Dentofacial Orthop* 92(3)*:*220-4.

Yu C, Abbott PV (2007). An overview of the dental pulp: its functions and responses to injury. *Aust Dent J* 52(1 Suppl)*:*S4-16.

Yu V, Damek-Poprawa M, Nicoll SB, Akintoye SO (2009). Dynamic hydrostatic pressure promotes differentiation of human dental pulp stem cells. *Biochem Biophys Res Commun* 386(4)*:*661-5.

Zhang W, Walboomers XF, Shi S, Fan M, Jansen JA (2006). Multilineage differentiation potential of stem cells derived from human dental pulp after cryopreservation. *Tissue Eng* 12(10)*:*2813-23.

# 9. CONCLUDING REMARKS

Twenty-eight, eight week old Sprague Dawley rats were divided into four groups of seven animals corresponding to one of four observations periods i.e.: $t_1$= 7 days, $t_2$= 14 days, $t_3$= 21 days, $t_4$= 28 days. At t=0 days, six animals in each group received a thermal insult, a continuous 20 minute application of dry ice ($CO_2$ at $-81^0$C) to the crowns of their upper right maxillary molar. The untreated left molars were used as controls. The remaining rat within each group did not receive the dry ice. Following sacrifice, the maxilla was dissected out, fixed in ethanol and embedded in methylmethacrylate. Ten microns thick, undecalcified maxillary first molar coronal sections through the furcation were obtained.

An issue in this research study was obtaining and mounting flat, intact sections. Many sections were torn and displayed loss of material. It was noted in all the torn sections, the specimen was not completely embedded with methylmethacrylate material. This was postulated to be due to the incomplete infiltration of the specimen with the embedding material. Material loss as a result of incomplete filtration may also be exacerbated during the sectioning process with the microtome. Manipulation of the already brittle section during the subsequent mounting of sections and staining further increased material loss. Occasionally, folds in sections had to be left in situ to minimize further loss. Cellular detail was not consistent across the sections. This may be related to the integrity of the sections as all rats received the same processing and staining protocol and the quality of the cellular detail did not appear to be related to the day of sacrifice or the stain type.

Chang[147] postulated that a longer period for the clearing and infiltration processes under vacuum may have been beneficial to optimizing embedding of the specimens.

Ankylosis seen in this study was characterized by a focal nodular region with thickening of mineralized tissue extending from both the bone and root surface into the PDL. The tomographic view provided by serial sections (Article 1, Figure 10) shows that ankylosis may occur in localised areas in three planes of space. This suggests that where ankylosis did occur, it appeared to be a spatially and temporally controlled event. The presence of inhibitory molecules within the central region of the periodontal ligament may have prevented complete mineralization of a wider zone of the PDL[2].

Only three out of the 24 experimental rats displayed definitive ankylosis. Another three rats at day 21 had morphological features of pronounced mineralized tissue deposition on the furcal root surface but no definite ankylotic bridge (Appendix 10.5). These were not included in the ankylosis sample as it was uncertain if these were an artefact due to the angle of the section creating the appearance of finger-like extension from bony trabeculae.

Compared to earlier studies[82, 83], there was a deceased incidence of ankylosis. Some factors, which were also postulated by Di Iulio[83], may have accounted for variability. These are: (1) Inter-rat variabilities in the thickness of dentine and/or enamel on the ground occlusal surface; (2) Tooth surface to which the dry ice pellets was applied. Dreyer[46] suggested the occlusal surface was the best surface for the application of the cold stimulus as better thermal conductivity occurs when the stimulus is applied parallel to the dentinal tubules. Due to the small size of the occlusal surface of the molars,

inadvertent differential buccal surface application may have occurred; (3) Inconsistency in the physical size of the pellets applied or replaced. This would have affected the surface area of contact with the tooth surface and thermal conductivity. Large pellets would have a diminished area of contact with the occlusal surface, with an increased air-insulating effect. During the 20 minute duration, the pellets had to be frequently replaced as they diminished in size from evaporation. Examination of the photos taken during dry ice application suggested that variabilities in physical size of the pellets applied may have partly explained the variations in the histological responses seen. Future studies using this model should take into consideration a method of standardizing the size of the dry ice pellets applied.

The severity of insult has been positively correlated with incidence of ankylosis[85]. Dreyer[46] found increased incidence of ankylosis in teeth which underwent longer and repeated applications of dry ice. Ankylosis was also present in the rat which displayed bone-like tissue within the pulp. This phenomenon was also noted in other studies using a tooth replantation model[147,148]. This suggests the need for a stronger noxious stimulus. Thus, based on the above studies and this study's findings, it is postulated that with a longer freezing period, the incidence, permanence and progressiveness of dentoalveolar ankylosis and mineral formation within the pulp would eventually be established.

The results of this study indicate that the mineral profile of ankylotic tissue is similar to that of bone. However, the small incidence of ankylosis found in this study creates difficulty in accurate comparisons to the surrounding hard tissues. The morphology of ankylotic tissue did not display any structural organisation when compared to bone and

dentine. This in conjunction with the focal, nodular appearance within the centre of the PDL suggests that ankylosis maybe a product of the osteogenic potential of PDL cells and that it is not similar to ankylotic bone.

Future research should aim at modifying the aseptic root resorption technique to improve the incidence of ankylosis. In particular further investigation of transient ankylosis as noted by Hammarström[85] may provide insight into the regulatory factors that play a role in the maintenance and homeostasis of the PDL. Little is known on the molecular basis of the initiation of ankylosis. It has been suggested that a balance in the activities of bone sialoprotein and osteopontin may contribute to maintaining an unmineralised PDL region[2]. The paravascular regions in rodents are a common region for fibroblast progenitors[3]. In this regard, the protective role of fibroblasts, as has been suggested in other studies, in particular the competing activities of RANK and osteoprotegerin for the RANK-L ligand, should be further investigated[26,7].

# 10. APPENDICES

## 10.1 SPECIMEN PREPARATION

### 10.1.1 Tissue Dehydration and Processing Protocol

The following procedure was used for the impregnation of tissues with methylmethacrylate. All the procedures below except the last stage occurred in a vacuum chamber. Each specimen was placed in individual 25ml polypropylene tubes. At the last stage, to facilitate polymerization of the methylmethacrylate, the polypropylene tubes were tightly sealed and placed in a water bath in a 37°C temperature regulated oven. For each time interval, the old solution was discarded and fresh solution replenished:

| | | |
|---|---|---|
| Fixation- | 70% ethanol | 1hr |
| Dehydration- | 70% ethanol | 4hours |
| | 70% ethanol | Overnight |
| | 85% ethanol | 4 hours |
| | 85% ethanol | 4 hours |
| | 85% ethanol | Overnight |
| | 95% ethanol | 4 hours |
| | 95% ethanol | 4 hours |
| | 95% ethanol | Overnight |
| | 100% ethanol | 4 hours |
| | 100% ethanol | 4 hours |
| | 100% ethanol | Overnight |

| | | |
|---|---|---|
| | 100% ethanol | 4 hours |
| | 100% ethanol | Overnight |
| Defat | 100% ethanol | 1 hour |
| | 100% ethanol | 1 hour |
| | Acetone | 24 hours |
| Infiltration | Methylmethacrylate monomer (MMA) | 5 days |
| | MMA+Hardener | 5 days |
| | MMA+Hardener+Initiator | 2-3 days |

The hardener was Polyethyleneglycol 400 added to MMA in the ratio of 1 part Polyethyleneglycol 400 and 10 parts MMA.

The initiator was Bis(4-tert-butyl cyclohexyl) peroxydicarbonate with a measured 0.4% (w/v of the combined volume of MMA+Hardener) in grams dissolved in the MMA+Hardener solution to commence initiation of polymerization.

## 10.2 SLIDE PREPARATION AND SECTION PROCESSING PROTOCOL

### 10.2.1 Slide coating procedures for undecalcified bone sections

All slides were coated with gelatine solution according to the following procedure. Pre-coating of slides facilitates adherence of sections. All slides were obtained pre-cleaned.

1. 10 grams of gelatine was dissolved in one litre of deionised water, heated to 60ºC and left to cool.

2. 1 gram of chromic potassium sulphate was then added with the assistance of a stirrer. This acted as an antifungal.
3. Place slides in racks
4. Each rack was placed in gelatine for a few seconds, then left on extraction overnight to dry.

### 10.2.2 Unstained sections- processing

**1.** Remove filter paper and plastic

**2.** Soak slides in acetone (using a Copland jar or slide rack) for 10-15 minutes to remove methyl methacrylate

**3.** Clear in 2 series of xylene and place coverslip with adhesive

### 10.2.3 Undecalcified sections- processing for VK/H&E staining

1. Repeat steps 1 and 2 in Appendix 3
2. Wash gently with distilled water 3x
3. Add 1% silver nitrate (made up in distilled water). This was made from stock 5% silver nitrate (stored at 4°C) with 1 part 5% silver nitrate and 4 parts distilled water.
4. Place slides in front of UV source for 1 hour. (the Copland jar or slide rack is rotated once or twice during this time.
5. Wash gently with distilled water 3x.
6. Add 2.5% sodium thiosulphate for 5 minutes. This is made from stock 5% sodium thiosulphate solution.

7. Wash gently with distilled water 3x.
8. Place slides in haematoxylin for 10 minutes
9. Wash in running tap water for 1 minute
10. Differentiate with acid alcohol (couple of dips)
11. Wash in running tap water for 1 minute
12. Blue in saturated lithium carbonate (25 seconds)
13. Rinse in running tap water (30 seconds)
14. Stain with eosin for 2-4 minutes
15. Dehydrate with a 2 series of 100% ethanol, clear with 2 series of xylene and place coverslip with adhesive

### 10.2.4 Decalcified sections- processing for H&E staining

1. Repeat steps 1 and 2 in Appendix 3
2. Repeat steps 7-15 in Appendix 4

### 10.2.5 Removing coverslips from unstained slides

1. Fill a large beaker with xylene (all procedures done in a fume hood)
2. Place slides in racks
3. Immerse racks in beaker
4. Leave and monitor for 4 days
5. If coverslips have not slid off, leave for another day or until all coverslips have been removed
6. Remove racks from xylene and allow to dry overnight.

## 10.3 EDS MEASUREMENT PROTOCOL

### 10.3.1 Scan Timing

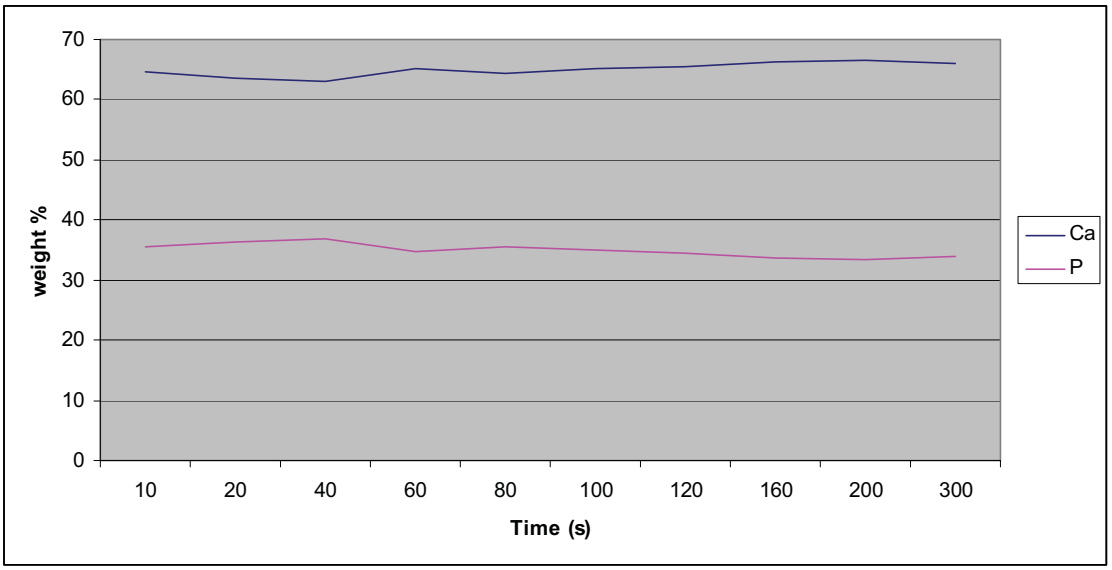


Weight percentages for Ca and P plotted over time. Fluctuations in readings reduced from 100s onwards. Thus 100s was taken as data acquisition time.

### 10.3.2 Calculating number of measurements per tissue required.

20 measurements were taken of dentine with the settings: 10kV, 100 live seconds.

| number of scans | ca/p ratio |
|---|---|
| 1 | 1.94 |
| 2 | 1.93 |
| 3 | 1.88 |
| 4 | 1.94 |
| 5 | 1.8 |
| 6 | 1.88 |
| 7 | 1.88 |
| 8 | 1.79 |
| 9 | 1.85 |
| 10 | 1.9 |
| 11 | 2 |
| 12 | 2.49 |
| 13 | 1.83 |
| 14 | 1.92 |
| 15 | 1.76 |
| 16 | 1.79 |
| 17 | 1.83 |
| 18 | 2.31 |
| 19 | 1.74 |
| 20 | 1.72 |

| | |
|---|---|
| **Mean** | 1.909 |
| **Standard Deviation** | 0.186 |
| **Coefficient of Variation (%)** | 9.721 |

A standard error of the Ca/P ratios was plotted vs. number of scans.

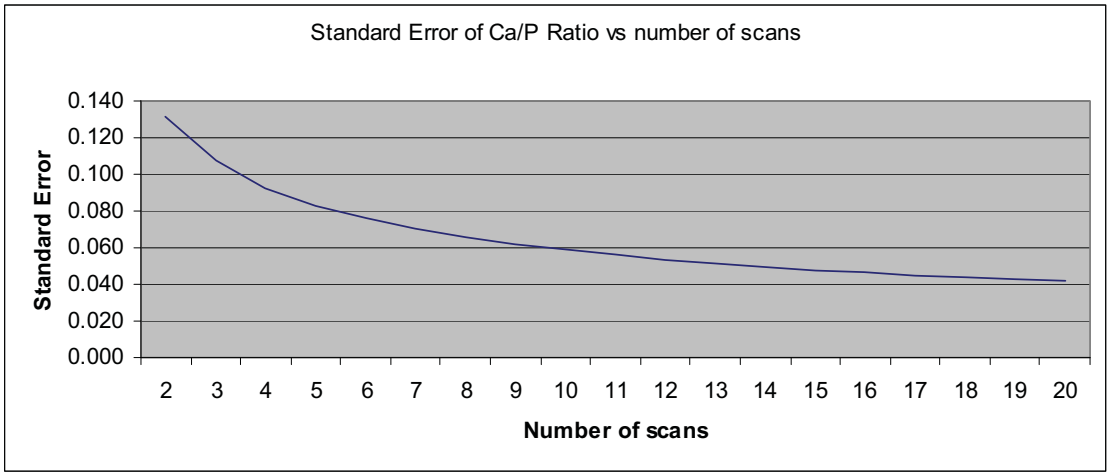


From the Standard error plot, there was not a lot of gain from taking more than 3 measures. With articles in literature taking 3-5 scans per tissue, it was decided that 3 measurements was reasonable (Huumonen, 1999; Tjaderhane, 1995).

## 10.4 STATISTICAL DATA

All calculations were performed using SAS Version 9.2 (SAS Institute Inc., Cary, NC, USA).

In assessing differences in minerals between teeth and across regions in the experimental rats, linear mixed effects models were fitted to the data. In the models side (left, right), region (bone, cementum, dentine, and ankylosis) and the interaction between side and region were included as fixed effects. A random animal effect was included in all the models so as to adjust for the dependence in results from the same animal. Where the interaction between side and region was found to be non-significant (i.e. $p > 0.05$), a second model excluding the interaction term was fitted to the data.

### 10.4.1 Phosphorus

| Type 3 Tests of Fixed Effects | | | | |
|---|---|---|---|---|
| Effect | Num DF | Den DF | F Value | P-value |
| Region | 3 | 104 | 1.56 | 0.2039 |
| Side | 1 | 104 | 0.64 | 0.4243 |
| Region*side | 2 | 104 | 3.51 | 0.0334 |

The table 'Type 3 Tests of Fixed Effects' shows the significance of the fixed effects (predictor variables) in the linear mixed effects model. Since this model includes an interaction term, the main effects of region and side do not need to be interpreted. The interaction between region and side was found to be statistically significant ($p = 0.0334$), suggesting that the difference between regions in mean phosphorus levels depended on the side of measurement (or alternatively that the difference between left and right sides depended on the region).

| Adjusted Means | | | | |
|---|---|---|---|---|
| Effect | Region | Side | Estimate | Standard Error |
| Region*side | a | r | 23.3808 | 0.6578 |
| Region*side | b | l | 23.8915 | 0.4303 |
| Region*side | b | r | 23.8984 | 0.4493 |
| Region*side | c | l | 24.0490 | 0.4386 |
| Region*side | c | r | 24.6605 | 0.5037 |
| Region*side | d | l | 24.2279 | 0.4302 |
| Region*side | d | r | 22.8375 | 0.4566 |

a = ankylosis, b = bone, c = cementum, d = dentine, l = left, r = right

The table 'Adjusted Means' shows the mean phosphorus levels for each combination of region and side as estimated by the linear mixed effects models (i.e. after adjusting for missingness and the clustering in the data). The table shows that the mean phosphorus level was fairly comparable between left and right sides for bone (23.89 vs. 23.90 for left and right sides respectively), whereas for cementum and dentine the left and right sides were more disparate. Note that you can use the adjusted means for plotting purposes if you like.

| Differences of Adjusted Means | | | | | | | | | |
|---|---|---|---|---|---|---|---|---|---|
| Effect | Region | Side | _ Region | _Side | Estimate | Standard Error | DF | t Value | P-value |
| Region*side | a | r | B | l | -0.5108 | 0.7132 | 104 | -0.72 | 0.4755 |
| Region*side | a | r | B | r | -0.5176 | 0.7196 | 104 | -0.72 | 0.4736 |
| Region*side | a | r | C | l | -0.6682 | 0.7164 | 104 | -0.93 | 0.3532 |
| Region*side | a | r | C | r | -1.2797 | 0.7667 | 104 | -1.67 | 0.0981 |
| Region*side | a | r | D | l | -0.8471 | 0.7133 | 104 | -1.19 | 0.2377 |
| Region*side | a | r | D | r | 0.5433 | 0.7278 | 104 | 0.75 | 0.4571 |
| Region*side | b | l | B | r | -0.00687 | 0.5290 | 104 | -0.01 | 0.9897 |
| Region*side | b | l | C | l | -0.1574 | 0.5180 | 104 | -0.30 | 0.7618 |
| Region*side | b | l | C | r | -0.7689 | 0.5765 | 104 | -1.33 | 0.1852 |
| Region*side | b | l | D | l | -0.3363 | 0.5125 | 104 | -0.66 | 0.5131 |
| Region*side | b | l | D | r | 1.0540 | 0.5353 | 104 | 1.97 | 0.0516 |
| Region*side | b | r | C | l | -0.1505 | 0.5334 | 104 | -0.28 | 0.7783 |
| Region*side | b | r | C | r | -0.7621 | 0.5839 | 104 | -1.31 | 0.1948 |
| Region*side | b | r | D | l | -0.3295 | 0.5289 | 104 | -0.62 | 0.5347 |
| Region*side | b | r | D | r | 1.0609 | 0.5419 | 104 | 1.96 | 0.0529 |
| Region*side | c | l | C | r | -0.6115 | 0.5805 | 104 | -1.05 | 0.2946 |
| Region*side | c | l | D | l | -0.1789 | 0.5197 | 104 | -0.34 | 0.7313 |
| Region*side | c | l | D | r | 1.2114 | 0.5396 | 104 | 2.24 | 0.0269 |
| Region*side | c | r | D | l | 0.4326 | 0.5763 | 104 | 0.75 | 0.4546 |
| Region*side | c | r | D | r | 1.8229 | 0.5898 | 104 | 3.09 | 0.0026 |
| Region*side | d | l | D | r | 1.3903 | 0.5351 | 104 | 2.60 | 0.0107 |

Since the interaction term was statistically significant I've presented post-hoc tests comparing combinations of side and region two at a time.

*Conclusions from model:*

Post-hoc tests revealed that the mean phosphorus level for dentine in the left side was on average 1.39 units higher than the mean level for dentine in the right side ($p = 0.0107$).

Post-hoc tests revealed that the mean phosphorus level for cementum on the left side was on average 1.21 units higher than the mean level for dentine on the left side ($p=1.2114$)

Post-hoc tests revealed that the mean phosphorus level for cementum on the right side was on average 1.82 units higher than mean level for dentine on the right side ($p=0.0026$)

### 10.4.2 Calcium

| Type 3 Tests of Fixed Effects | | | | |
|---|---|---|---|---|
| Effect | Num DF | Den DF | F Value | P-value |
| Region | 3 | 104 | 1.61 | 0.1921 |
| Side | 1 | 104 | 0.00 | 0.9942 |
| Region*side | 2 | 104 | 2.19 | 0.1170 |

| Adjusted Means | | | | |
|---|---|---|---|---|
| Effect | Region | Side | Estimate | Standard Error |
| Region*side | a | r | 44.9851 | 2.2102 |
| Region*side | b | l | 47.7490 | 1.4169 |
| Region*side | b | r | 47.9691 | 1.4827 |
| Region*side | c | l | 44.4285 | 1.4460 |
| Region*side | c | r | 47.1146 | 1.6743 |
| Region*side | d | l | 46.7849 | 1.4166 |
| Region*side | d | r | 43.8547 | 1.5090 |

The interaction effect was not statistically significant ($p = 0.1170$), thus we do not have evidence to conclude that calcium levels depended on the combination of region and side. In order to be able to interpret the main effects of region and side, a second linear mixed effects model excluding the interaction term was fitted to the data.

| Type 3 Tests of Fixed Effects | | | | |
|---|---|---|---|---|
| Effect | Num DF | Den DF | F Value | P-value |
| Region | 3 | 106 | 1.58 | 0.1974 |
| Side | 1 | 106 | 0.02 | 0.9019 |

| Adjusted Means | | | | |
|---|---|---|---|---|
| Effect | Region | Side | Estimate | Standard Error |
| Region | a | | 45.1337 | 2.2977 |
| Region | b | | 47.8653 | 1.1324 |
| Region | c | | 45.5344 | 1.2015 |
| Region | d | | 45.4249 | 1.1405 |
| Side | | l | 46.0582 | 1.1453 |
| Side | | r | 45.9210 | 1.0561 |

There was no evidence for a difference in mean calcium levels between the four regions ($p = 0.1974$) or between the right and left sides ($p = 0.9019$). Note that since there was no overall difference between the four regions I have not presented any post hoc tests comparing the regions two at a time.

*Conclusions from model:*
The model demonstrated that mean calcium levels did not depend on the combination of region and side (interaction p-value = 0.12). A second model excluding the interaction term revealed no differences in mean calcium levels between the four regions ($p = 0.20$) or between right and left sides ($p = 0.90$).

### 10.4.3 Calcium/Phosphate Ratio

| Type 3 Tests of Fixed Effects | | | | |
|---|---|---|---|---|
| Effect | Num DF | Den DF | F Value | P-value |
| Region | 3 | 104 | 3.29 | 0.0235 |
| Side | 1 | 104 | 0.40 | 0.5278 |
| Region*side | 2 | 104 | 0.21 | 0.8145 |

| Adjusted Means | | | | |
|---|---|---|---|---|
| Effect | Region | Side | Estimate | Standard Error |
| Region*side | a | r | 1.9109 | 0.06320 |
| Region*side | b | l | 1.9899 | 0.03961 |
| Region*side | b | r | 2.0010 | 0.04153 |
| Region*side | c | l | 1.8495 | 0.04047 |
| Region*side | c | r | 1.8994 | 0.04733 |
| Region*side | d | l | 1.9218 | 0.03960 |
| Region*side | d | r | 1.9225 | 0.04237 |

The interaction effect was not statistically significant ($p = 0.81$), thus we do not have evidence to conclude that calcium levels depended on the combination of region and side. In order to be able to interpret the main effects of region and side, a second linear mixed effects model excluding the interaction term was fitted to the data.

| Type 3 Tests of Fixed Effects | | | | |
|---|---|---|---|---|
| Effect | Num DF | Den DF | F Value | P-value |
| Region | 3 | 106 | 3.49 | 0.0182 |
| Side | 1 | 106 | 0.35 | 0.5557 |

| Adjusted Means | | | | |
|---|---|---|---|---|
| Effect | Region | Side | Estimate | Standard Error |
| Region | a | | 1.9018 | 0.06486 |
| Region | b | | 1.9957 | 0.03015 |
| Region | c | | 1.8719 | 0.03225 |
| Region | d | | 1.9228 | 0.03041 |
| Side | | l | 1.9136 | 0.03046 |
| Side | | r | 1.9326 | 0.02747 |

After adjusting for side, there was evidence for a significant difference between the four regions (p = 0.0182). The post-hoc tests comparing the regions are posted below.

| Differences of Adjusted Means | | | | | | | |
|---|---|---|---|---|---|---|---|
| Effect | Region | _Region | Estimate | Standard Error | DF | t Value | P-value |
| Region | a | b | -0.09391 | 0.06876 | 106 | -1.37 | 0.1749 |
| Region | a | c | 0.02992 | 0.07049 | 106 | 0.42 | 0.6721 |
| Region | a | d | -0.02102 | 0.06910 | 106 | -0.30 | 0.7616 |
| Region | b | c | 0.1238 | 0.03926 | 106 | 3.15 | 0.0021 |
| Region | b | d | 0.07289 | 0.03784 | 106 | 1.93 | 0.0568 |
| Region | c | d | -0.05094 | 0.03949 | 106 | -1.29 | 0.1999 |

The post-hoc tests revealed that the mean Ca/P ratio was significantly higher for bone than for cementum (difference = 0.1238, p = 0.0021).

### 10.4.4 Magnesium

| Type 3 Tests of Fixed Effects | | | | |
|---|---|---|---|---|
| Effect | Num DF | Den DF | F Value | P-value |
| Region | 3 | 104 | 51.89 | <.0001 |
| Side | 1 | 104 | 0.24 | 0.6268 |
| Region*side | 2 | 104 | 1.15 | 0.3204 |

| Adjusted Means | | | | |
|---|---|---|---|---|
| Effect | Region | Side | Estimate | Standard Error |
| Region*side | a | r | 0.7594 | 0.05807 |
| Region*side | b | l | 0.7819 | 0.03627 |
| Region*side | b | r | 0.7937 | 0.03797 |
| Region*side | c | l | 0.9713 | 0.03709 |
| Region*side | c | r | 0.8877 | 0.04351 |
| Region*side | d | l | 0.4498 | 0.03627 |
| Region*side | d | r | 0.4758 | 0.03890 |

The interaction effect was not statistically significant (p = 032), thus we do not have evidence to conclude that calcium levels depended on the combination of region and side. In order to be able to interpret the main effects of region and side, a second linear mixed effects model excluding the interaction term was fitted to the data.

| Type 3 Tests of Fixed Effects | | | | |
|---|---|---|---|---|
| Effect | Num DF | Den DF | F Value | P-value |
| Region | 3 | 106 | 53.43 | <.0001 |
| Side | 1 | 106 | 0.15 | 0.6989 |

| Adjusted Means | | | | |
|---|---|---|---|---|
| Effect | Region | Side | Estimate | Standard Error |
| Region | a | | 0.7642 | 0.06015 |
| Region | b | | 0.7871 | 0.02630 |
| Region | c | | 0.9351 | 0.02839 |
| Region | d | | 0.4613 | 0.02661 |
| Side | | l | 0.7430 | 0.02631 |
| Side | | r | 0.7309 | 0.02269 |

After adjusting for side, there was evidence for a significant difference between the four regions (p = <.0001).

| Differences of Adjusted Means | | | | | | | |
|---|---|---|---|---|---|---|---|
| Effect | Region | _Region | Estimate | Standard Error | DF | t Value | P-value |
| Region | a | b | -0.02288 | 0.06576 | 106 | -0.35 | 0.7286 |
| Region | a | c | -0.1709 | 0.06705 | 106 | -2.55 | 0.0122 |
| Region | a | d | 0.3029 | 0.06598 | 106 | 4.59 | <.0001 |
| Region | b | c | -0.1480 | 0.03856 | 106 | -3.84 | 0.0002 |
| Region | b | d | 0.3258 | 0.03730 | 106 | 8.73 | <.0001 |
| Region | c | d | 0.4738 | 0.03875 | 106 | 12.23 | <.0001 |

The post-hoc tests revealed that the mean value of mg was significantly lower for ankylosis than for cementum (difference = -0.1709, p = 0.0021).

### 10.4.5 Sodium

| Type 3 Tests of Fixed Effects | | | | |
|---|---|---|---|---|
| Effect | Num DF | Den DF | F Value | P-value |
| Region | 3 | 104 | 24.63 | <.0001 |
| Side | 1 | 104 | 0.95 | 0.3321 |
| Region*side | 2 | 104 | 0.97 | 0.3813 |

| Adjusted Means | | | | |
|---|---|---|---|---|
| Effect | Region | Side | Estimate | Standard Error |
| Region*side | a | r | 0.6432 | 0.06988 |
| Region*side | b | l | 0.4751 | 0.04533 |
| Region*side | b | r | 0.5165 | 0.04738 |
| Region*side | c | l | 0.4954 | 0.04623 |
| Region*side | c | r | 0.4663 | 0.05327 |
| Region*side | d | l | 0.7478 | 0.04532 |
| Region*side | d | r | 0.8360 | 0.04817 |

The interaction term was not statistically significant and so was removed from the model.

| Type 3 Tests of Fixed Effects | | | | |
|---|---|---|---|---|
| Effect | Num DF | Den DF | F Value | P-value |
| Region | 3 | 106 | 24.10 | <.0001 |
| Side | 1 | 106 | 1.15 | 0.2862 |

After adjusting for side, there was evidence for a significant difference between the four regions (p = <.0001).

| Adjusted Means | | | | |
|---|---|---|---|---|
| Effect | Region | Side | Estimate | Standard Error |
| Region | a | | 0.6231 | 0.07193 |
| Region | b | | 0.4954 | 0.03662 |
| Region | c | | 0.4864 | 0.03869 |
| Region | d | | 0.7899 | 0.03686 |
| Side | | l | 0.5804 | 0.03703 |
| Side | | r | 0.6171 | 0.03447 |

| Differences of Adjusted Means | | | | | | | |
|---|---|---|---|---|---|---|---|
| Effect | Region | _Region | Estimate | Standard Error | DF | t Value | P-value |
| Region | a | b | 0.1278 | 0.07363 | 106 | 1.74 | 0.0856 |
| Region | a | c | 0.1367 | 0.07567 | 106 | 1.81 | 0.0737 |
| Region | a | d | -0.1668 | 0.07404 | 106 | -2.25 | 0.0264 |
| Region | b | c | 0.008946 | 0.04152 | 106 | 0.22 | 0.8298 |
| Region | b | d | -0.2945 | 0.03994 | 106 | -7.37 | <.0001 |
| Region | c | d | -0.3035 | 0.04178 | 106 | -7.26 | <.0001 |

The post-hoc tests revealed that the mean value of Na was significantly lower in ankylosis than for dentine (difference = -0.1668, p = 0.0264).

The post-hoc tests revealed that the mean value of Na was significantly higher in bone compared to dentine (difference = -0.2945, p = <.0001).

The post-hoc tests revealed that the mean value of Na was significantly higher cementum compared to dentine (difference = 0.04178, p = <.0001).

## 10.5 IMAGES OF RATS WITH PARTIAL CHANGES WITHIN PDL

At day 21, 3 additional rats (rat ID 1, 4 and 5) had morphological features of pronounced mineralized tissue deposition on the furcal root surface but no definite ankylotic bridge.

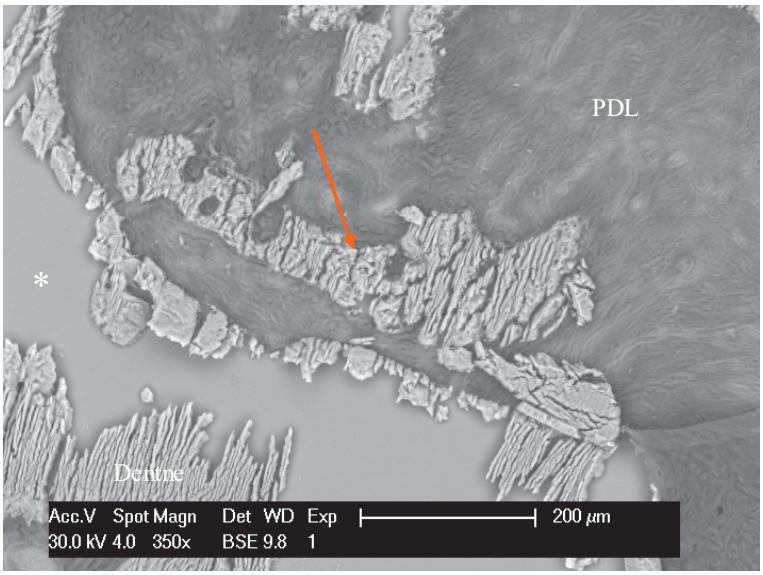


**Day 21, Rat 1. BSE image.** Mineralised bone-like tissue within the periodontal ligament (red arrow). A large tear features in the dentine region (asterix). Bone-like tissue was not observed on neighbouring slides. Thus maybe an artefact from slide preparation.

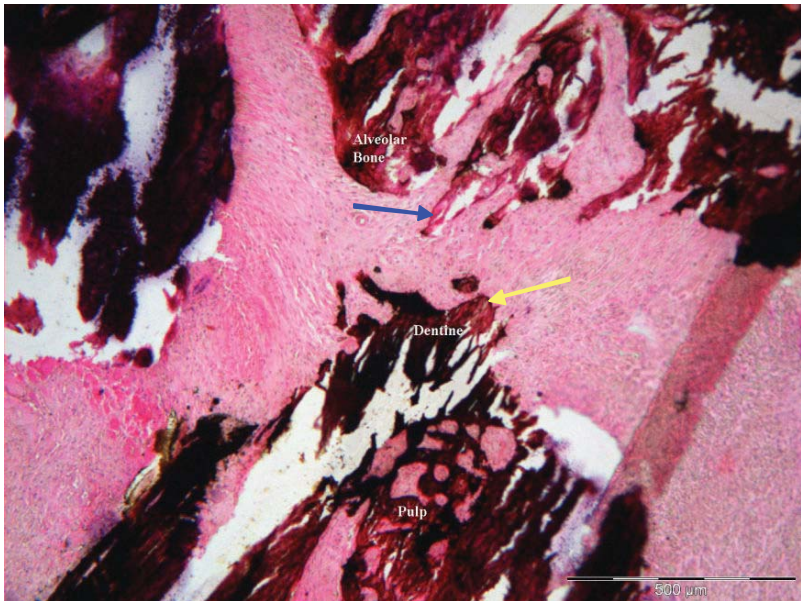


**Day 21, Rat 4. VK/H&E Stain**. Cementum-like deposits on the root surface (yellow arrow). Finger-like projections from alveolar bone (blue arrow). Scale bar 500µm.

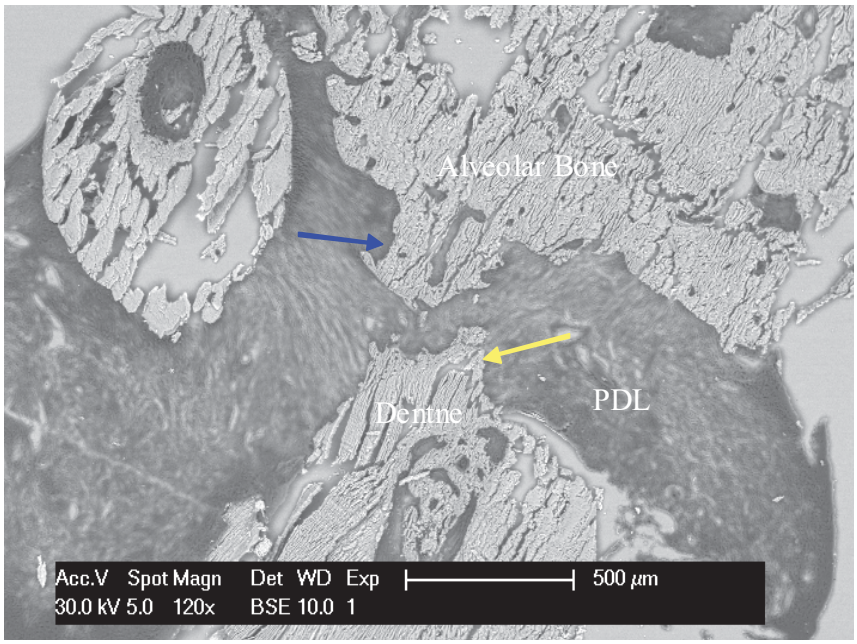


**Day 21, Rat 4. BSE image.** Cementum-like deposits on the root surface (yellow arrow). Bony projection from alveolar bone is visible (blue arrow). However, no ankylotic bridging observed.


**Day 21, Rat 5. H&E stain.** Reactive hard tissue thickening on tooth side of PDL.